Accepted Manuscript

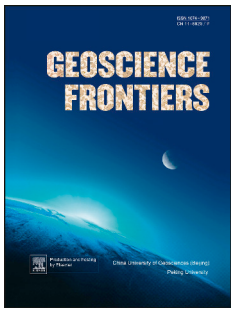

Tracking the Cretaceous transcontinental Ceduna River through Australia: The hafnium isotope record of detrital zircons from offshore southern Australia

Jarred Lloyd, Alan.S. Collins, Justin.L. Payne, Stijn Glorie, Simon Holford, Anthony.J. Reid

PII: S1674-9871(15)00062-6

DOI: 10.1016/j.gsf.2015.06.001

Reference: GSF 362

To appear in: *Geoscience Frontiers*

Received Date: 5 February 2015

Revised Date: 25 May 2015

Accepted Date: 1 June 2015

Please cite this article as: Lloyd, J., Collins, A.S., Payne, J.L., Glorie, S., Holford, S., Reid, A.J., Tracking the Cretaceous transcontinental Ceduna River through Australia: The hafnium isotope record of detrital zircons from offshore southern Australia, *Geoscience Frontiers* (2015), doi: 10.1016/j.gsf.2015.06.001.

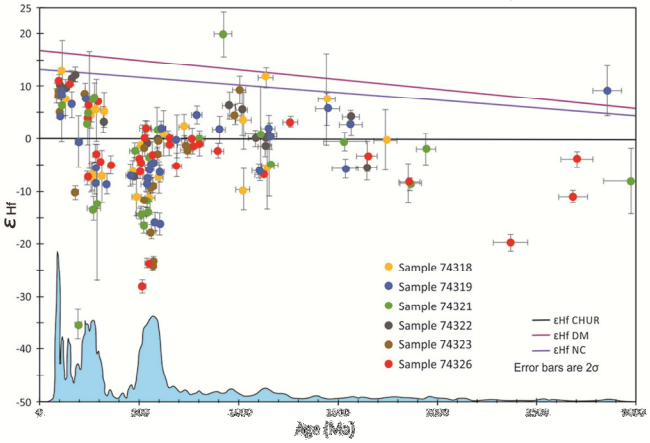

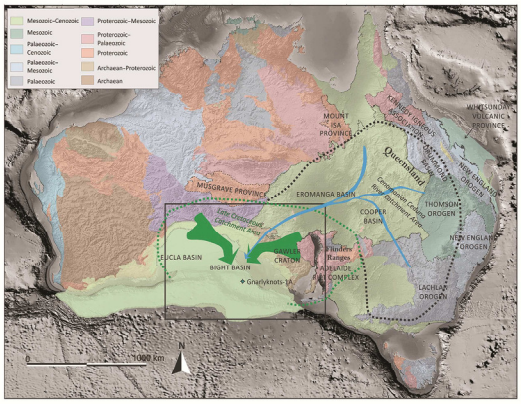

Tracking the Cretaceous transcontinental Ceduna River through Australia: The hafnium isotope record of detrital zircons from offshore southern Australia

Jarred Lloyd [a], Alan S. Collins [a,*], Justin L. Payne [b], Stijn Glorie [a], Simon Holford [c], Anthony J. Reid [d]

[a] *Centre for Tectonics, Resources and Exploration (TRaX), Department of Earth Sciences, The University of Adelaide, Adelaide, SA 5005, Australia*

[b] *Centre for Tectonics, Resources and Exploration (TRaX), School of Built and Natural Environments, The University of South Australia, GPO Box 2471 Adelaide, SA 5001 Australia*

[c] *Centre for Tectonics, Resources and Exploration (TRaX), Australian School of Petroleum, The University of Adelaide, Adelaide, SA 5005, Australia*

[d] *Geological Survey of South Australia, Department of State Development, Government of South Australia*

* Corresponding author. E-mail: alan.collins@adelaide.edu.au

Abstract

The middle–upper Cretaceous Ceduna River system traversed continental Australia from the NE coast to the centre of the southern coast. At its mouth, it formed a vast delta system that is similar in scale to the Niger delta of West Africa. The delta system is composed of two main lobes that represent different phases of delta construction. A recent hypothesis has challenged the traditional idea that both lobes of the delta were derived from a transcontinental river system by suggesting that the upper lobe (Santonian–Maastrichtian)

is instead derived from a restricted catchment within southern Australia. Hafnium isotopic data presented here fingerprint the original source of the upper delta lobe zircons to NE Australia, with data comparing well with similar U-Pb and Lu-Hf isotopic data from the Lachlan Orogen, the New England Orogen, the eastern Musgraves Province and the northern Flinders Ranges. These data do not preclude a model where the lobe is derived from recycled Eromanga Basin sediments during a phase of Late Cretaceous inland Australian uplift, but when coupled with reconnaissance low-temperature thermochronometry from the region of the Ceduna River course indicating widespread Triassic–Jurassic exhumation, and comparisons with detrital zircon data from the Winton Formation upstream of any proposed uplift, we suggest that both lobes of the Ceduna Delta are likely to be derived from a transcontinental Ceduna River.

Keywords: Detrital zircon; Hafnium; U-Pb; Ceduna sub-basin; Bight Basin; Australia

1. Introduction

The southern margin of Australia formed during the protracted separation of Australia from Antarctica that involved Jurassic-Cretaceous intra-East Gondwana rifting, followed by final separation along the central southern Australia margin by ca. 83.5 Ma in the Campanian (Krassay and Totterdell, 2003; Williams et al., 2011). This break-up of the last vestige of Gondwana led to the formation of the largest preserved delta system in Australia, covering an area of ca. 126,000 km^2 and found off the continent's southern coast (Figs. 1 and 2). The delta is thought to be sourced from a now-extinct transcontinental river system that traversed the continent in the middle to late Cretaceous from its distributary channel at the middle south coast, near the town of Ceduna, to its headwaters that are now found in central and northeast Australia (Veevers, 2000; Macdonald et al., 2013)(Figs. 1 and 2). Yet

much is controversial and unknown about the evolution of this river system. Particular controversy surrounds the temporal change in source areas over the time of the delta system's existence and the timing and process of exhumation of central Australia—the catchment area of the river system.

The Ceduna Sub-basin (Fig. 2) is the main depocentre in the large Bight Basin off the southern Australian coast. It contains two deltaic sequences that have been identified using seismic interpretation (Macdonald et al., 2012); a lower Cenomanian delta, represented by the White Pointer Supersequence, consisting of the Platypus and lower Wigunda Formations, and an overlying Santonian to Maastrichtian delta composed of the Hammerhead Supersequence, which contains the Potoroo and upper Wigunda Formations. Gnarlyknots-1A is an offshore well (Figs. 1 and 2) that preserves the best record of retrieved core available from the basin. This well forms the most complete succession available to study, yet it only penetrated the upper delta (the Hammerhead Supersequence).

Previous studies have suggested that both deltas were derived from a SW-flowing trans-continental river system that was sourced from the NE – either from the immediately older to contemporaneous Eromanga Basin (King and Mee, 2004)(Fig. 1), or from the NE coastal region of Australia (Queensland, Veevers, 2000). Macdonald et al. (2013) argued that the lower delta may well be sourced from Queensland, but they suggested that a phase of uplift associated with renewed rifting of Australia from Antarctica in the late Cretaceous rejuvenated the river system and that the upper delta was sourced from a much reduced catchment area within a NW–SE arc stretching from the Flinders Ranges to the Musgrave Province (Fig. 1).

Here we present new hafnium isotopic data from detrital zircons, whose U-Pb age data have been, for the most part, previously published (Macdonald et al., 2013). The Hf isotopic data are compared with comparable data from elsewhere in central and eastern Australia to better fingerprint the source region of this highly explorative sedimentary basin.

2. Analytical methods

2.1. Zircon U-Pb Geochronology

Existing U-Pb data from Macdonald et al. (2013) were used to recalculate the Hf isotopic data back to the formation of the individual zircon domains analysed in this study. This was possible because the same grains were analysed for Hf in this study that were analysed for U-Pb in Macdonald et al. (2013). In addition, extra U-Pb data were obtained from sample 74322 to increase the dataset. These data were obtained on a Laser Ablation Inductively Coupled Plasma Mass Spectrometry (LA-ICP-MS) using a New Wave UP-213 laser attached to an Agilent 7500cx Inductively Coupled Plasma Mass Spectrometer (ICP-MS) at Adelaide Microscopy, The University of Adelaide. Analysed zircons had been previously imaged under cathodoluminescence in both this study and in Macdonald et al. (2013). A laser spot size of 30 µm and repetition rate of 5 Hz was used for U-Pb analyses. Age calculations and corrections were completed using the software GLITTER with use of the primary zircon standard GJ-1, TIMS normalization data $^{207}Pb/^{206}Pb$ = 608.3 Ma, $^{206}Pb/^{238}U$ = 600.7 Ma and $^{207}Pb/^{235}U$ = 602.2 Ma (Jackson et al., 2004). Instrument drift was corrected for in GLITTER via standard bracketing every 15–20 unknowns and application of a linear correction.

Accuracy of the methodology was verified by repeated analyses of Plešovice zircon ($^{206}Pb/^{238}U$ = 337.13 ± 0.37 Ma; Sláma et al., 2008). Isotope ratios are presented uncorrected for common lead, with Concordia plots generated using Isoplot 4.15.

Kernel density estimates, probability density plots and histograms were all plotted using Density Plotter, a Java program developed by and described in Vermeesch (2012). An adaptive bandwidth was used for the kernel density estimates. A fixed age range of 0–3500 Ma and histogram bin width of 100 Ma was used for consistency across all plots. Data used were ±10% concordant.

2.2. Zircon Lu-Hf isotope analyses

In situ LA-MC-ICPMS Lu-Hf isotope analyses were carried out at the University of Adelaide facility using a New Wave Research 193 nm Excimer laser attached to a Neptune multi-collector ICP-MS system as per Payne et al (2013). Only grains with U–Pb ages having ≤ 10% discordance were analysed for Lu–Hf isotope composition. Analysis locations were in the same spot as concordant U–Pb spots. The bulk of analyses were carried out using a beam diameter of ~50 µm for large and a minimum of ~25 µm for smaller grains. Typical ablation times were 40–100 seconds using 5 Hz repetition rate, 4 ns pulse rate, and an intensity of ~10 J/cm^2. Zircons were ablated in a helium atmosphere, which was then mixed with argon upstream of the ablation cell.

Analyses used a dynamic measurement routine with ten 0.524 s integrations on ^{171}Yb, ^{173}Yb, ^{175}Lu, ^{176}Hf (+Lu + Yb), ^{177}Hf, ^{178}Hf, ^{179}Hf and ^{180}Hf, one 0.524 s integration on ^{160}Gd, ^{163}Dy, ^{164}Dy, ^{165}Ho, ^{166}Er, ^{167}Er, ^{168}Er, ^{170}Yb and ^{171}Yb, and one 0.524 s integration of Hf oxides with masses ranging from 187 to 196 amu. An idle time of 1.5 s was included between each mass

change to allow for magnet settling and to negate any possible effects of signal decay. The measurement cycle was repeated 15 times providing a total maximum measurement time of 3.75 min including an off-peak baseline measurement. Hf oxide formation rates for all analytical sessions in this study were in the range 0.1–0.07%. Hf mass bias was corrected using an exponential fractionation law with a stable $^{179}Hf/^{177}Hf$ ratio of 0.7325. Yb and Lu isobaric interferences on ^{176}Hf were corrected for following the methods of Woodhead et al. (2004). ^{176}Yb interference on ^{176}Hf was corrected for by direct measurement of Yb fractionation using measured $^{171}Yb/^{173}Yb$ with the Yb isotopic values of Segal et al. (2003). The applicability of these values were verified by analysing JMC 475 Hf solutions doped with varying levels of Yb with interferences up to $^{176}Yb/^{177}Hf = \sim 0.5$. ^{176}Lu isobaric interference on ^{176}Hf was corrected using a $^{176}Lu/^{175}Lu$ ratio of 0.02655 (Vervoort et al., 2004) assuming the same mass bias behaviour as Yb. Confirmation of accuracy of the technique was monitored using the Plešovice, Mudtank and Temora II zircon standards. Mean $^{176}Hf/^{177}Hf$ values for each standard along with the published values are given in Supplementary Table 2. $\varepsilon Hf(T)$, and T_{DM} crustal were calculated using the ^{176}Lu decay constant after Scherer et al. (2001). T_{DM} crustal was calculated using the methods of Griffin et al. (2002) with an average crustal composition of $^{176}Lu/^{177}Hf = 0.015$.

3. Results

3.1 Additional U-Pb Zircon Data Gnarlyknots-1A Sample 74322

A further 55 zircon U-Pb data were acquired from sample 74322, sampled from the Turonian to Santonian Wigunda Formation to increase the number of data available from this sample. The analysed grains were selected without using any particular criteria, to avoid

undue bias in the data collection. Fifty three of the data are within 10% of concordance (Supplementary Table 1, Fig. 3). The new data complement the existing data of Macdonald et al. (2013), with a few data yielding Mesoarchaean-Neoarchaean ages, some 1800–2100 Ma detritus, late Mesoproterozoic ages, a minor concentration in the Tonian–Cryogenian, major detrital peaks in the Ediacaran–Cambrian and Carboniferous–Triassic and a final concentration of Cretaceous-aged detritus. The youngest concordant $^{206}Pb/^{238}U$ age is 98.0 ± 2.6 Ma (2σ error), which is slightly older than the maximum depositional age of 91.3 ± 3.2 Ma reported from this sample in Macdonald et al. (2013), consistent with the sample being Turonian–Santonian in age.

3.2 Hafnium Isotope Data from Gnarlyknots-1A

Corrected εHf(t) values from Gnarlyknots-1A are given in Fig. 4. Lu-Hf isotope ratios were taken from samples 74318, 74319, 74321, 74322, 74323 and 74326 and as shown, all samples yield large variations in age corrected εHf values, ranging from highly evolved (–46.4) to very juvenile (+19.9). There are distinct and diffuse populations in the dataset that correspond to the U-Pb age populations that, in a number of cases, distinguish between similar-aged populations, emphasizing the importance of obtaining Hf isotope data where possible to distinguish between source regions.

With one exception, all 3000–2300 Ma zircons show negative εHf(t) values indicating evolved sources for those zircons. The exception is a zircon (ca. 2859 Ma, second oldest zircon of the sample) with a highly positive εHf(t) value that demonstrates a juvenile source for this grain. There is a broad trend of less negative values with increasing age in this population with εHf(t) values ranging from –19.6 to +9.1, suggesting that younger Archaean zircons may have crystallised from reworked Mesoarchaean crust. A second population at ca. 2000–1400 Ma,

with εHf(t) values ranging from +7.4 to –8.4, has an inverse trend from the Archaean examples with increasingly negative values with increasing age, suggesting a greater involvement of the Mantle in the source magmas.

Late Mesoproterozoic zircons (ca. 1260–1080 Ma) appear to show two subpopulations, both of similar age. One population consists of zircons with moderately evolved εHf(t) values (–6.7 to –5.0), whilst the second population is characterised by near zero εHf(t) values (–1.5 to +1.9). This suggests two different zircon sources. One zircon (ca. 1139 Ma) has an εHf(t) value of +11.7, indicating a highly juvenile source.

Zircons spanning the Mesoproterozoic-Neoproterozoic boundary, between ca. 1030-895 Ma, show generally positive εHf values. This suggests more Mantle involvement in the source magma. Epsilon Hf values range from –9.6 to +19.7 although most values lie between –1.8 and +9.3.

Zircon grains dated between the Cryogenian and the Ordovician (ca. 800–450 Ma) make up ca. 40% of the total analysed zircons. The older zircons in this population (ca. 800–650 Ma) plot about the zero εHf line, broadly between +5 and –3. After ca. 650 and until ca. 455 Ma, many zircons show a vertical spread between about +2.1 and highly evolved values down to –17.5. There is also a smaller population of ca. 570–513 Ma zircons with highly negative values (–28 to –23.3).

Silurian and Devonian zircons are absent, but Carboniferous to Lower Jurassic zircons (~360–180 Ma) form two distinct εHf(t) populations. An evolved population (εHf(t) = –13.3 to –3) of ca. 360-180 Ma zircons and a second population that overlaps in age (ca. 320–200 Ma), but generally younger than the previous population, has moderately juvenile εHf(t) values range from –0.6 to +8.5 with most falling between +3 and +8.5.

A final population of lower Jurassic–Cretaceous zircons (ca. 180–95 Ma) contains moderate to highly juvenile εHf(t) values (+4.3 to +12.8). Within this population a tight grouping (approx. 74%) of juvenile zircons occur between ca. 130 Ma and ca. 95 Ma.

4. Discussion

4.1. U-Pb Age Provenance of Upper Ceduna Delta

The 620 U-Pb data now available from ≤10% concordant detrital zircons from the Gnarlyknots-1A core (from Macdonald et al., 2013 and this study)(Fig. 3) show the limited input of Archaean and Palaeoproterozoic detritus in the delta, despite the proximity of rocks with similar crystallisation ages exposed close to the delta distributary channel in the Gawler Craton (Hand et al., 2007; Reid and Hand, 2012). This suggests that much of the adjacent margin wasn't exposed in the Santonian to Maastrichtian, or at least that the part of the Ceduna River that traversed the Gawler Craton wasn't erosional over this part of its path, at that time. The first sizable peak in detrital ages occurs at ca. 1150–1100 Ma. This is older than many of the Musgraves Province granites, but does overlap with the younger end of magmatism in this area (Smithies et al., 2011; Kirkland et al., 2013). Similar-aged inherited zircons (xenocrysts) have been reported within the Phanerozoic granites that intrude the Lachlan Orogen of southeast and east Australia (Kemp et al., 2006). The Palaeozoic sedimentary country rocks to these intrusions are also rich in similar-aged zircon detritus that is thought to be sourced from Antarctica, or elsewhere in Gondwana (Squire et al., 2006). There is an age minimum at approximately 1050 Ma with an increase back to zircons with Tonian and Cryogenian ages (Fig. 3). Granitic igneous rocks of this age are rare in

Australia, but again, inherited and detrital zircons of this age are common within later granites and metasedimentary rocks in the Lachlan Orogen (Kemp et al., 2006; Squire et al. 2006) and also from Cryogenian to Palaeozoic sedimentary rocks from the Centralian Superbasin (Maidment et al., 2007). The first really major concentration of detrital zircon ages occurs in the Ediacaran–Cambrian (Fig. 3), which overlaps with magmatism in the Adelaide Rift Complex (Foden et al., 2006) and is reflected by similar-aged detrital zircons, and inherited zircons in the Lachlan Orogen (Kemp et al., 2006; Squire et al., 2006; Fergusson et al., 2013) and in the Centralian Superbasin (Maidment et al., 2007). There is a significant lack of detrital zircon ages through the Silurian, Devonian and Carboniferous, despite the frequency of granites of this age found in the Lachlan Orogen. The next major zircon age peak records Permian and Triassic ages. Granitoid magmatism of this age is only found exposed in Australia in the New England Orogen of east and northeast Australia (Fig. 1)(Phillips et al., 2011; Chisholm et al., 2014; Jeon et al., 2014). Further U-Pb detrital zircon ages occur in the Late Jurassic to middle Cretaceous, coeval with voluminous silicic volcanism in eastern Australia (including the ca. 135–95 Ma Whitsunday Silicic LIP; Bryan et al., 2012)(Fig. 1). These findings are similar to those suggested by Tucker et al. (2013, 2014) and Macdonald et al. (2013).

4.2. Provenance Implications of Hafnium Isotope Data

The hafnium isotopic record, of the same zircons whose U-Pb ages are discussed above, adds an independent data set to help evaluate the provenance of the Gnarlyknots-1A sandstone samples. When the measured Hf isotopes are corrected for the crystallisation ages of the zircon (and therefore the age at which the Hf was trapped in the zircon), and normalised to the Chondrite Uniform Reservoir (CHUR) and plotted against its age, the

resulting figure (Fig. 4) reveals some interesting trends. These temporal isotopic trends reflect the evolution of magmas, in which the detrital zircons originally grew, within the source regions. The main age trends have been discussed in the results section above; here we discuss their similarity, or dissimilarity, to comparable data from eastern and south-central Australia that form possible source regions (Figs. 1 and 5).

Limited Archaean data are available from the Gnarlyknots-1A zircons, but the general decrease in εHf(t) values with decreasing age, noted above, is broadly reflected in the inherited zircon data from SE Australian granites (Kemp et al., 2006)(Fig. 5). Late Palaeoproterozoic–early Mesoproterozoic data from Gnarlyknots-1A are similar in hafnium isotopic values to those seen in the Mount Painter region (northern Flinders Ranges) of South Australia (Figs. 1 and 5)(Kromkhun et al., 2013), and from the eastern part of the Musgraves Province (Smits et al., 2014), which bound the suggested catchment area of the Ceduna River to both sides (Fig. 1). Stenian zircons may be sourced from the Musgraves Province of central Australia, or recycled from the Lachlan Orogen of SE Australia. The εHf(t) versus Age plot shows that although there is overlap between the Gnarlyknots-1A data and the younger zircons from the Musgraves (Smithies et al., 2011; Kirkland et al., 2013), the more evolved zircons are outside the Musgraves trend, but do overlap with coeval zircons from the Lachlan Orogen (Kemp et al., 2006)(Fig. 5), suggesting that these might be more likely source for these grains. The prominent trend of decreasing age and decreasing εHf(t) values between ca. 1000 and 600 Ma is also broadly mirrored in the Lachlan Orogen granites inherited zircon data, as is the marked shift to evolved values in the Ediacaran (Kemp et al., 2006)(Fig. 5). Kemp et al. (2009) recorded hafnium isotopic data for many Palaeozoic granites in the Lachlan Orogen, equivalent-aged zircons from Gnarlyknots-1A are noticeable by their absence (Fig. 5). This may be because these data come predominantly from the south of the Lachlan Orogen, away from the probable headwaters of the Ceduna River system. We suggest that older, inherited zircons in the granites better

represent the detrital zircons in the surrounding sedimentary rocks, which are the country rocks to the Palaeozoic granites, and were presumably were entrained in the granites as xenocrysts. These sedimentary rocks form much of the Lachlan and Thompson Orogens of eastern Australia and appear to have been eroded and recycled into the Ceduna River system, whereas zircons that crystallised in the granites, which are more numerous in the southern parts of the orogeny, did not.

Permian and Triassic detritus in the Upper Ceduna delta fall into two distinct fields, a slightly older evolved group and a more juvenile group. The juvenile group overlaps well with data from the New England Orogen (Jeon et al., 2014; Phillips et al., 2011; Tucker, 2014), although data from the New England Batholith does stretch to much more juvenile values than recorded in zircons from Gnarlyknots-1A (Phillips et al., 2011)(Fig. 5). The more evolved zircon population may be sourced from the Kennedy Igneous Association (Champion and Bultitude, 2013) of central and northern Queensland. No hafnium data are available from these Carboniferous-Permian (ca. 345–260 Ma) extrusive and intrusive rocks, but neodymium isotope data yield evolved values (Champion and Bultitude, 2013). Finally, late Jurassic–middle Cretaceous detrital zircon overlaps with similar data collected from the Cretaceous Mackunda and Winton Formations in Queensland (Tucker, 2014), the upper part of the latter formation has recently been dated as being deposited in the Turonian, with the single youngest concordant zircon dated at 92.5 Ma (Tucker et al., 2013), coeval with the upper delta in the Ceduna Sub-basin.

4.3. Constraints on the Ceduna River System and the Evolution of Central Australia

The provenance data presented here support the original origin of detrital zircons found today in the Turonian to Maastrichtian part of the Ceduna Delta system to lie in NE Australia, in Queensland (broadly the area outlined as the ‘Cenomanian Ceduna River

Catchment Area' in Fig. 1)(Bryan et al. 1997; Veevers, 2000). These correlate with Turonian to Santonian mudstones and deltaic sandstones overlain by a voluminous Santonian to Maastrichtian delta lobe (Macdonald et al., 2012). U-Pb and Hf detrital zircon data are consistent with similar data from the inherited zircons in granites from SE Australia (Kemp et al., 2006), granites from the New England Orogen and the Kennedy Igneous Association (Phillips et al., 2011; Champion and Bultitude, 2013; Jeon et al., 2014; Tucker, 2014), from the far north Flinders Ranges and the eastern Musgraves Province (Kromkhun et al., 2013; Smits et al., 2014) and from the coeval Winton Formation of the uppermost Eromanga Basin (Tucker, 2014), which was undisputably sourced from N and E Queensland, based on palaeocurrent and detrital heavy mineral data (Bryan et al. 1997; Tucker et al. 2013). An ultimate source from NE Australia does not, however, disprove the hypothesis of Macdonald et al. (2013), who argued that the Upper Ceduna Delta (Santonian to Maastrichtian) was sourced from a relatively restricted catchment, largely in the present state of South Australia (see Fig. 1). They argued this based largely on zircon fission track data from southern Australia that show considerable exhumation in the Upper Cretaceous. In this model, the 'Queensland'-provenance of many of the Ceduna delta zircons would remain valid because they were recycled from the lower Cretaceous formations within the Eromanga Basin.

A caveat to this model is that, unlike coastal Australia, there is very little fission track, or other low-temperature thermochronological data available from inland Australia; especially from the proposed catchment of the Ceduna River through northern South Australia and southwestern Queensland. The results of a reconnaissance study from the central Gawler craton has recently been published (Reddy et al., 2015) that encompasses a region close to

any putative course of the Ceduna River. This study yielded apatite fission track and U-Th-Sm/He ages indicating that this region did not experience major cooling and exhumation after the Triassic-Jurassic (ca. 230–190 Ma). Only one sample yielded younger apatite fission track ages of ca. 130–100 Ma (Reddy et al., 2015). These data are sparse, but tantalizingly suggest that at least the central Gawler Craton was exhumed before the Late Cretaceous, and that any Late Cretaceous river that traversed this region was unlikely to have caused widespread erosion. Post-Jurassic thermal events, captured in the thermochronological record of the Gawler Craton are interpreted as the result of partial resetting by a combination of shallow burial beneath the Eromanga Basin and flow of elevated temperature groundwater within the Eromanga aquifer system (Gleadow et al., 2002; Reddy et al., 2015) that is also seen in the underlying Cooper Basin (Middleton et al. 2014). These data contrast with new information from the Drummond Basin of Queensland, which lies closer to the proposed headwaters of the Ceduna River system (Fig. 1). Here, modelled (U-Th)/He apatite and zircon data suggest a phase of rapid exhumation at ca. 80 Ma (Zhang et al., 2014). In addition to this lack of evidence of late Cretaceous cooling (and therefore presumably exhumation) along the course of the Ceduna River system, away from its headwaters, a new maximum depositional age of ca. 92.5 Ma on the Winton Formation in central Queensland (Tucker et al., 2013), suggests that this part of the Winton Formation (at least) post-dates the Cenomanian Lower Ceduna Delta lobe and is coeval with at least the mixed deltaic/fore-delta mudstones that underlie the main Santonian to Maastrichtian Upper Ceduna Delta lobe (Macdonald et al., 2012). Taken together, these observations suggest that both delta lobes may be deposited from river systems that originated in Cretaceous Queensland. However, more low-temperature thermochronological data are needed both from central Australia, and from detrital minerals in the resulting basins, to

truly track the exhumation of Australia and follow the source to sink history of the fill of the extensive Australian Mesozoic basins.

5. Conclusions

Hafnium isotope data from zircons from Turonian to Maastrichtian sandstones within the Upper Ceduna Delta in the Bight Basin, southern Australia, suggest that the ultimate provenance of many of the zircons in this delta are from NE Australia, in the region of the exposed New England Orogen and the Whitsunday Silicic LIP of Queensland. The data presented here do not solve the debate about whether the 'Queensland-origin zircons' in the Santonian-Maastrichtian upper delta lobe were recycled from the Eromanga Basin during a late Cretaceous pulse of uplift and exhumation as proposed by Macdonald et al. (2013), but correlation with the Winton Formation in Queensland and new reconnaissance low-temperature thermochronological data from the central Gawler Craton (Reddy et al., 2015), suggest that this is not necessary and that the transcontinental Ceduna River is likely to have existed throughout the Cretaceous.

Acknowledgements

Jarred Lloyd undertook this work as part of an Honours project at University of Adelaide, in part funded by the Geological Survey of South Australia. Aoife McFadden and Ben Wade (Adelaide Microscopy) are thanked for assistance obtaining CL images and in collecting U-Pb data. This paper forms TRAX Record #326 and is an output of ARC Future Fellowship grant FT120100340 and IGCP projects #628 and #648. Scott Bryan and an anonymous reviewer are thanked for their thorough reviews that considerably improved the paper.

Figure Captions

Figure 1

Digital Elevation Map of Australia and its continental shelf with the broad ages of exposed geology indicated. The dotted lines indicate the proposed different catchment areas of the Cenomanian lower Ceduna Delta (black dotted line) and the Santonian-Maastrichtian upper Ceduna Delta (green dotted line)(modified from Macdonald et al., 2013). Location of Fig. 2 is indicated by the box.

Figure 2

The Ceduna Sub-basin of the Bight Basin off the coast of southern Australia. The location of the Gnarlyknots-1A well is indicated as is the town of Ceduna, close to the inferred Cretaceous location of the delta distributary channel. Inset is a schematic log of the Gnarlyknots-1A well with the location of the samples indicated (log modified from Macdonald et al., 2013).

Figure 3

Combined probability density distribution, kernel density estimate plots and histograms of U-Pb age data from the Gnarlyknots-1A well that samples the Turonian-Maastrichtian succession within the central Ceduna Sub-basin. Plotted with the program 'Density Plotter' (Vermeesch, 2012). The $^{207}Pb/^{206}Pb$ age is used for zircons older than 1000 Ma, whilst the

$^{206}Pb/^{238}U$ age is used for younger analyses due to the different half-lives of the parent uranium isotopes.

Figure 4

Hafnium isotopic data, presented as $\varepsilon Hf(t)$ values, versus age. The light blue curve below is the kernel density estimate presented in Fig. 4 to indicate relative abundance of age populations. CHUR = Chondrite Universal Reservoir (Bouvier et al., 2008), DM = Depleted Mantle (Vervoort and Blichert-Toft, 1999); NC = New Crust (Hawkesworth et al., 2010).

Figure 5

Epsilon Hf(*t*) versus age plot of data presented in this study (black dots) comparing with similar data from eastern and central Australia. Grey fields are data from the Musgraves Province presented in Smits et al. (2014), dark grey equates to the majority of the data, whereas the light grey fields are field of more sparse data.

Supplementary Table 1

U-Pb data for sample 74322.

Supplementary Table 2

Hf isotope data of samples from the Turonian to Maastrichtian Gnarlyknocks-1a well.

Supplementary Figure

U-Pb Concordia plot of new detrital zircon data from sample 74322 from the Turonian to Santonian Wigunda Formation. Data point error ellipses are at 2 standard deviations.

References

Bouvier, A., Vervoort, J.D., Patchett, P.J., 2008. The Lu-Hf and Sm-Nd isotopic composition of CHUR: Constraints from unequilibrated chondrites and implications for the bulk composition of terrestrial planets. Earth and Planetary Science Letters 273, 48-57.

Bryan, S.E., Constantine, A.E., Stephens, C.J., Ewart, A., Schön, R.W., Parianos, J., 1997. Early Cretaceous volcano-sedimentary successions along the eastern Australian continental margin: Implications for the break-up of eastern Gondwana. Earth and Planetary Science Letters 153, 85-102.

Bryan, S.E., Cook, A.G., Allen, C.M., Siegel, C., Purdy, D.J., Greentree, J.S., Uysal, I.T., 2012. Early-mid Cretaceous tectonic evolution of eastern Gondwana: From silicic LIP magmatism to continental rupture. Episodes 35, 142-152.

Champion, D.C., Bultitude, R.J., Kennedy Igneous Association, in Jell, P.A. (Ed.), Geology of Queensland pp. 473-514.

Chisholm, E.-K., Blevin, P., Simpson, C., 2014. New SHRIMP U–Pb zircon ages from the New England Orogen, New South Wales, p. 248.

Fergusson, C.L., Nutman, A.P., Kamiichi, T., Hidaka, H., 2013. Evolution of a Cambrian active continental margin: The Delamerian-Lachlan connection in southeastern Australia from a zircon perspective. Gondwana Research 24, 1051-1066.

Foden, J., Elburg, M.A., Dougherty-Page, J., Burtt, A., 2006. The timing and duration of the Delemerian Orogeny: correlation with the Ross Orogen and implications for Gondwana assembly. Journal of Geology 114, 189-210.

Gleadow, A.J.W., Kohn, B.P., Brown, R.W., O'Sullivan, P.B., Raza, A., 2002. Fission track thermotectonic imaging of the Australian continent. Tectonophysics 349, 5-21.

Griffin, W.L., Wang, X., Jackson, S.E., Pearson, N.J., O'Reilly, S.Y., Xu, X., Zhou, X., 2002. Zircon chemistry and magma mixing, SE China: In-situ analysis of Hf isotopes, Tonglu and Pingtan igneous complexes. Lithos 61, 237-269.

Hand, M., Reid, A., Jagodzinski, L., 2007. Tectonic framework and evolution of the Gawler craton, southern Australia. Economic Geology 102, 1377-1395.

Hawkesworth, C.J., Dhuime, B., Pietranik, A.B., Cawood, P.A., Kemp, A.I.S., Storey, C.D., 2010. The generation and evolution of the continental crust. Journal of the Geological Society 167, 229-248.

Jackson, S.E., Pearson, N.J., Griffin, W.L., Belousova, E.A., 2004. The application of laser ablation-inductively coupled plasma-mass spectrometry to in-situ U/Pb zircon geochronology. Chemical Geology 211, 47-69.

Jeon, H., Williams, I.S., Bennett, V.C., 2014. Uncoupled O and Hf isotopic systems in zircon from the contrasting granite suites of the New England Orogen, eastern Australia:

Implications for studies of Phanerozoic magma genesis. Geochimica et Cosmochimica Acta 146, 132-149.

Kemp, A.I.S., Hawkesworth, C.J., Collins, W.J., Gray, C.M., Blevin, P.L., EIMF, 2009. Isotopic evidence for rapid continental growth in an extensional accretionary orogen: The Tasmanides, eastern Australia. Earth & Planetary Science Letters 284, 455-466.

Kemp, A.I.S., Hawkesworth, C.J., Paterson, B.A., Kinny, P.D., 2006. Episodic growth of the Gondwana supercontinent from hafnium and oxygen isotopes in zircon. Nature 439, 580-583.

King, S.J., Mee, B.C., 2004. The seismic stratigraphy and petroleum potential of the Late Cretaceous Ceduna Delta, Ceduna Sub-basin, Great Australian Bight, in: Boult, P.J., Johns, S.D., Lang, S.C. (Eds.), Eastern Australasian Basins Symposium II. . Petroleum Exploration Society of Australia, Special Publication, pp. 63–73.

Kirkland, C.L., Smithies, R.H., Woodhouse, A.J., Howard, H.M., Wingate, M.T.D., Belousova, E.A., Cliff, J.B., Murphy, R.C., Spaggiari, C.V., 2013. Constraints and deception in the isotopic record; the crustal evolution of the west Musgrave Province, central Australia. Gondwana Research 23, 759-781.

Krassay, A.A., Totterdell, J.M., 2003. Seismic stratigraphy of a large, Cretaceous shelf-margin delta complex, offshore southern Australia. Aapg Bull 87, 935-963.

Kromkhun, K., Foden, J., Hore, S., Baines, G., 2013. Geochronology and Hf isotopes of the bimodal mafic-felsic high heat producing igneous suite from Mt Painter Province, South Australia. Gondwana Research 24, 1067-1079.

Maidment, D.W., Williams, I.S. and Hand, M., 2007. Testing long-term patterns of basin sedimentation by detrital zircon geochronology,Centralian Superbasin, Australia. Basin Research 19, 335-360.

Macdonald, J., Backé, G., King, R., Holford, S., Hillis, R., In:, (eds), 2012. Geomechanical modelling of fault reactivation in the Ceduna Sub-basin, Bight Basin, Australia, in: Healy, D., Butler, R.W.H., Shipton, Z.K., Sibson, R.H. (Eds.), Faulting, Fracturing and Igneous Intrusion in the Earth's Crust. Geological Society, London, Special Publications, pp. 71–89.

Macdonald, J.D., Holford, S.P., Green, P.F., Duddy, I.R., King, R.C., Backe, G., 2013. Detrital zircon data reveal the origin of Australia's largest delta system (vol 170, pg 3, 2013). Journal of the Geological Society 170, 379-379.

Middelton, A.W., Uysal, I.T., Bryan, S.E., Hall, C.M., Golding, S.D., 2014. Integrated 40Ar-39Ar, 87Rb-87Sr and 147Sm-143Nd geochronology of authigenic illite to evaluate tectonic reactivation in an intraplate setting, central Australia. Geochimica et Cosmochimica Acta 134, 155-174.

Payne, J.L., Pearson, N.J., Grant, K.J., Halverson, G.P., 2013. Reassessment of relative oxide formation rates and molecular interferences on in situ lutetium-hafnium analysis with laser ablation MC-ICP-MS. Journal of Analytical Atomic Spectrometry 28, 1068-1079.

Phillips, G., Landenberger, B., Belousova, E.A., 2011. Building the New England Batholith, eastern Australia-Linking granite petrogenesis with geodynamic setting using Hf isotopes in zircon. Lithos 122, 1-12.

Reddy, M., Glorie, S., Reid, A., Collins, A.S., 2015. Phanerozoic cooling history of the central Gawler Craton: implications of new low- temperature thermochronological data. MESA Journal.

Reid, A.J., Hand, M., 2012. Mesoarchean to Mesoproterozoic evolution of the southern Gawler Craton, South Australia. Episodes 35, 216-225.

Scherer, E., Münker, C., Mezger, K., 2001. Calibration of the lutetium-hafnium clock. Science 293, 683-687.

Segal, I., Halicz, L., Platzner, I.T., 2003. Accurate isotope ratio measurements of ytterbium by multi-collector inductively coupled plasma mass spectrometry applying erbium and hafnium in an improved double external normalisation procedure. Journal of Analytical Atomic Spectrometry 18, 1217-1223.

Sláma, J., Kosler, J., Condon, D.J., Crowley, J.L., Gerdes, A., Hanchar, J.M., Horstwood, M.S.A., Morris, G.A., Nasdala, L., Norberg, N., Schaltegger, U., Schoene, B., Tubrett, M.N., Whitehouse, M.J., 2008. Plesovice zircon - A new natural reference material for U-Pb and Hf isotopic microanalysis. . Chemical Geology 249, 1-35.

Smithies, R.H., Howard, H.M., Evins, P.M., Kirkland, C.L., Kelsey, D.E., Hand, M., Wingate, M.T.D., Collins, A.S., Belousova, E., 2011. High-Temperature Granite Magmatism, Crust-Mantle Interaction and the Mesoproterozoic Intracontinental Evolution of the Musgrave Province, Central Australia. Journal of Petrology 52, 931-958.

Smits, R.G., Collins, W.J., Hand, M., Dutch, R., Payne, J., 2014. A Proterozoic Wilson cycle identified by Hf isotopes in central Australia: Implications for the assembly of Proterozoic Australia and Rodinia. Geology 42, 231-234.

Squire, R.J., Campbell, I.H., Allen, C.M., Wilson, C.J.L., 2006. Did the Transgondwanan Supermountain trigger the explosive radiation of animals on Earth? Earth and Planetary Science Letters 250, 116-133.

Tucker, R., 2014. Stratigraphy, sedimentation and age of the upper Cretaceous Winton Formation, central-western Queensland, Australia: implications for regional palaeogeography, palaeoenvironments and Gondwana palaeontology. James Cook University, p. 228.

Tucker, R.T., Roberts, E.M., Hu, Y., Kemp, A.I.S., Salisbury, S.W., 2013. Detrital zircon age constraints for the Winton Formation, Queensland: Contextualizing Australia's Late Cretaceous dinosaur faunas. Gondwana Research 24, 767-779.

Veevers, J.J., 2000. Billion-year Earth History of Australiaand Neighbours in Gondwanaland. GEMOC Press, Sydney.

Vermeesch, P., 2012. On the visualisation of detrital age distributions. Chemical Geology 312-313, 190-194.

Vervoort, J.D., Blichert-Toft, J., 1999. Evolution of the depleted mantle: Hf isotope evidence from juvenile rocks through time. Geochimica et Cosmochimica Acta 63, 533-556.

Vervoort, J.D., Patchett, P.J., Soderlund, U., Baker, M., 2004. Isotopic composition of Yb and the determination of Lu concentrations and Lu/Hf ratios by isotope dilution using MC-ICPMS. Geochemistry Geophysics Geosystems 5.

Williams, S.E., Whittaker, J.M., Muller, R.D., 2011. Full-fit, palinspastic reconstruction of the conjugate Australian-Antarctic margins. Tectonics 30.

Woodhead, J.D., Hergt, J.M., Shelley, M., Eggins, S., Kemp, R., 2004. Zircon Hf-isotope analysis with an Excimer laser, depth profiling, ablation of complex geometries, and concomitant age estimation. . Chemical Geology 209, 121-135.

Zhang, W., Min, K.K., Bryan, S.E., 2014. Thermal History of Drummond Basin, Queensland (Australia) from Apatite and Zircon (U-Th)/He Thermochornology. Abstract V43D-4923 presented at 2014 Fall Meeting, AGU, San Francisco, Calif., 15-19 Dec.

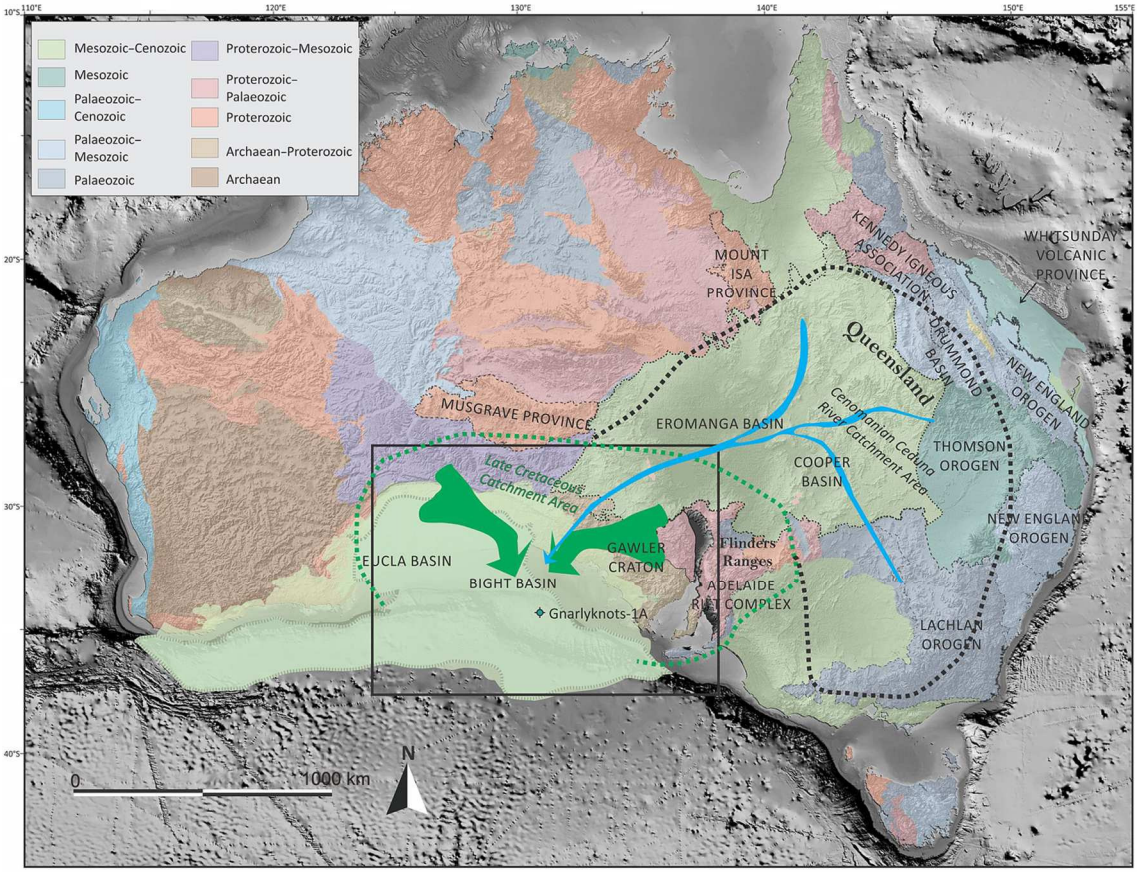

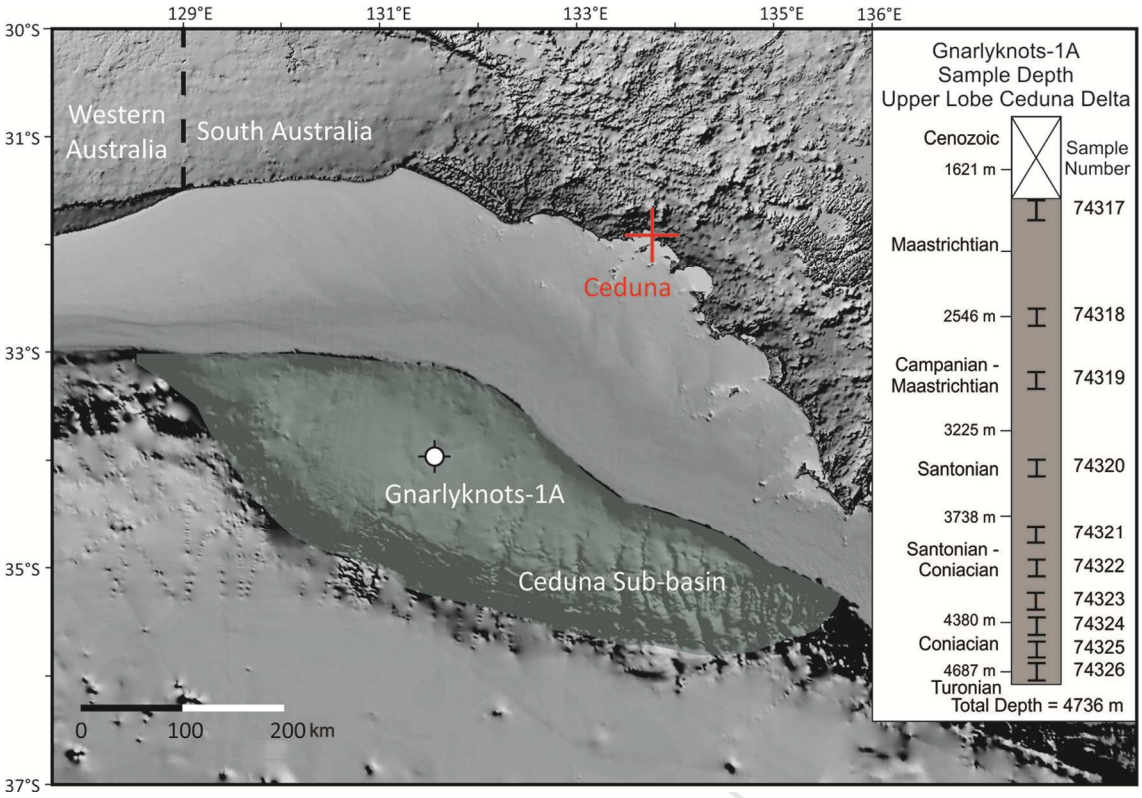

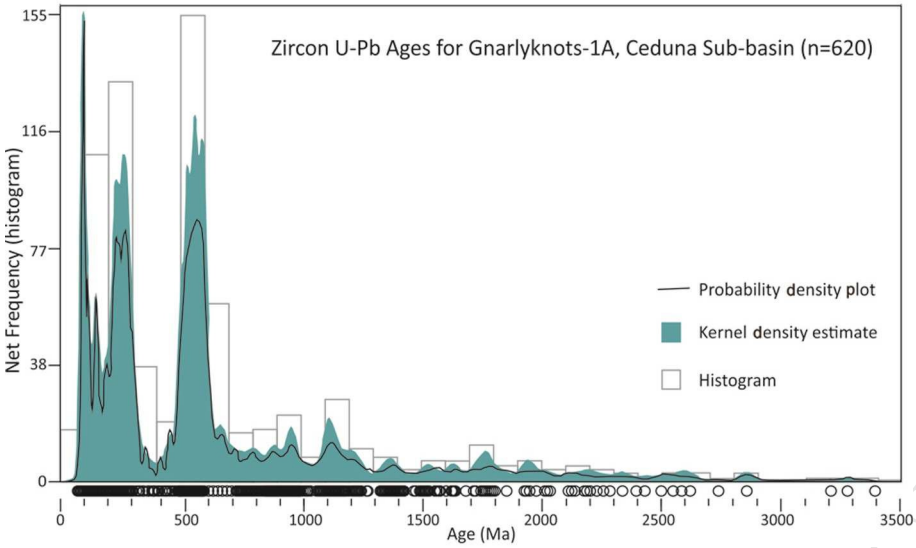

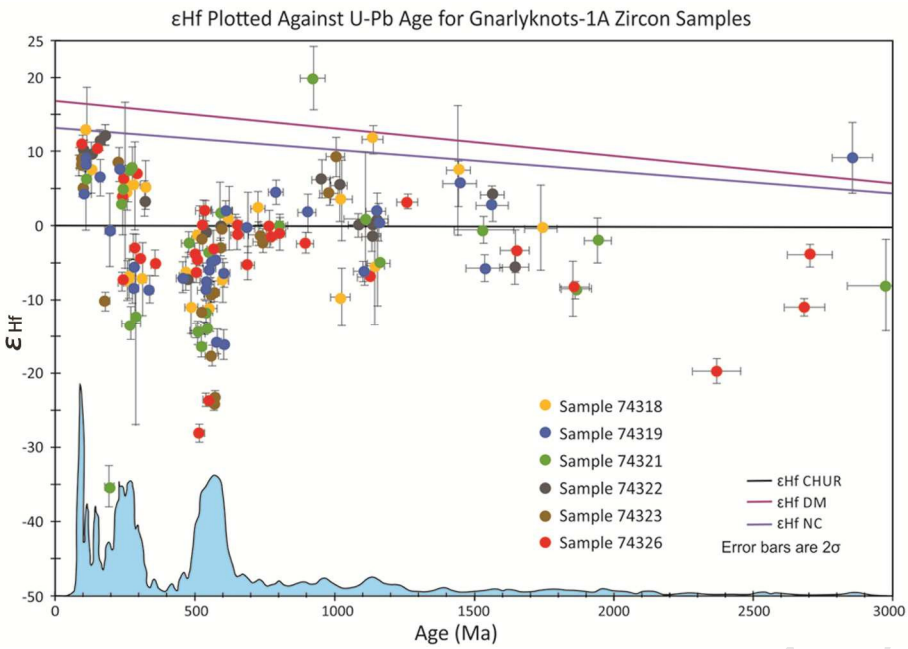

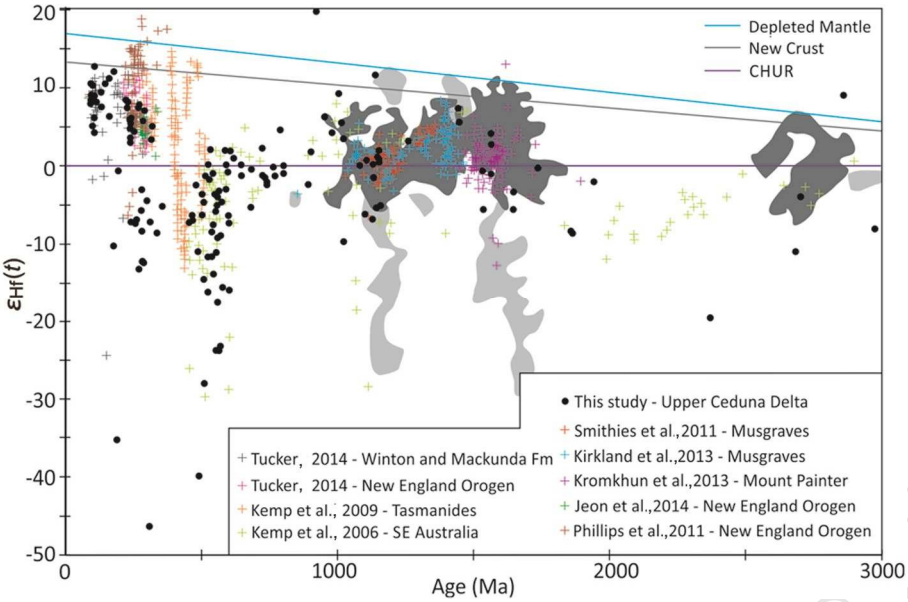

Highlights

- Ceduna Delta Hf zircon data show a provenance from NE Australia
- Zircon εHf(t) data suggest a source component recycled from the Lachlan Orogen
- Considerable zircon from the Whitsunday Silicic LIP survives <1000 km transport
- The Santonian–Maastrichtian Upper Delta is likely sourced from a transcontinental river system

	Isotopic ratios								Age			
Analysis	Pb207/Pb206	1σ err	Pb207/U235	1σ err	Pb206/U238	1σ err	Rho	Conc.	Pb207/Pb206	1σ err	Pb206/U238	1σ err
74322_081	0.04821	0.00267	0.10176	0.00555	0.01531	0.00028	0.12	100	109.8	125.76	98	1.77
74322_082	0.11576	0.00143	5.12815	0.07453	0.32142	0.00433	0.61	102	1891.8	22.04	1796.6	21.11
74322_083	0.04974	0.00162	0.11160	0.00363	0.01628	0.00025	0.23	103	183.1	73.97	104.1	1.61
74322_084	0.05637	0.00107	0.73263	0.01472	0.09431	0.00134	0.43	96	466.2	41.83	581	7.91
74322_085	0.06933	0.00095	1.47415	0.02326	0.15428	0.00211	0.58	99	908.7	28.07	924.9	11.8
74322_086	0.05125	0.00104	0.34838	0.00743	0.04933	0.00071	0.41	98	252.1	46.01	310.4	4.36
74322_087	0.05292	0.00236	0.13092	0.00576	0.01795	0.00031	0.16	109	325.3	98	114.7	1.99
74322_088	0.06029	0.00137	0.75234	0.01768	0.09055	0.00136	0.37	102	614.1	48.39	558.8	8.01
74322_089	0.15512	0.00225	6.06968	0.09964	0.28395	0.00405	0.56	123	2403.1	24.44	1611.2	20.31
74322_090	0.06261	0.00167	0.63145	0.01704	0.07318	0.00116	0.31	109	695.1	56	455.3	6.99
74322_091	0.08375	0.00122	2.32230	0.03885	0.20121	0.00284	0.57	103	1286.6	28.26	1181.8	15.22
74322_092	0.05639	0.00158	0.34467	0.00977	0.04436	0.00071	0.30	107	466.8	61.39	279.8	4.36
74322_093	0.06023	0.00091	0.79887	0.01378	0.09624	0.00136	0.55	101	611.8	32.31	592.4	8.01
74322_094	0.05004	0.00139	0.24642	0.00699	0.03573	0.00056	0.31	99	197	63.35	226.3	3.47
74322_095	0.12315	0.00177	5.66719	0.09500	0.33389	0.00476	0.58	104	2002.3	25.32	1857.2	23.02
74322_096	0.05486	0.00127	0.26540	0.00642	0.03510	0.00054	0.38	107	406.3	50.78	222.4	3.36
74322_097	0.08193	0.00119	2.11357	0.03552	0.18714	0.00273	0.58	104	1243.9	28.16	1105.9	14.84
74322_098	0.06178	0.00097	0.82967	0.01479	0.09742	0.00142	0.55	102	666.7	33.26	599.3	8.36
74322_099	0.05896	0.00950	0.75052	0.11666	0.09234	0.00446	0.04	100	565.8	316.82	569.4	26.32
74322_100	0.05121	0.00123	0.26416	0.00662	0.03742	0.00058	0.38	101	250.5	54.46	236.8	3.6
74322_101	0.05035	0.00166	0.26257	0.00868	0.03784	0.00064	0.26	99	211	74.57	239.4	3.96
74322_102	0.05073	0.00175	0.13295	0.00459	0.01901	0.00032	0.25	104	228.6	77.62	121.4	2.03
74322_103	0.06380	0.00095	1.03168	0.01784	0.11732	0.00172	0.58	101	734.9	31.18	715.1	9.93
74322_104	0.13210	0.00161	7.05382	0.10813	0.38740	0.00560	0.67	100	2126.1	21.22	2110.8	26.01
74322_105	0.20450	0.00249	15.68730	0.24034	0.55654	0.00806	0.67	100	2862.4	19.63	2852.3	33.4
74322_106	0.11069	0.00152	3.82243	0.06290	0.25054	0.00370	0.62	111	1810.8	24.75	1441.3	19.06
74322_107	0.06823	0.00107	1.27169	0.02297	0.13523	0.00202	0.56	102	875.4	32.24	817.6	11.45
74322_108	0.08945	0.00122	2.97702	0.04904	0.24145	0.00355	0.62	101	1413.8	25.79	1394.2	18.46
74322_109	0.10112	0.00127	3.86792	0.06099	0.27750	0.00405	0.66	102	1644.9	23.15	1578.7	20.41
74322_110	0.07835	0.00119	2.10357	0.03730	0.19478	0.00292	0.58	100	1155.8	29.89	1147.2	15.74

74322_111	0.07223	0.00499	1.75283	0.11664	0.17605	0.00486	0.11	98	992.5	134.36	1045.3	26.64
74322_112	0.05113	0.00088	0.30024	0.00583	0.04261	0.00064	0.53	99	246.5	39.08	269	3.97
74322_113	0.04991	0.00384	0.10764	0.00810	0.01565	0.00038	0.09	104	190.8	169.85	100.1	2.42
74322_114	0.16678	0.00232	10.86797	0.18335	0.47272	0.00710	0.62	101	2525.6	23.17	2495.5	31.1
74322_115	0.05711	0.00132	0.64343	0.01571	0.08173	0.00130	0.41	100	495.2	50.62	506.4	7.78
74322_116	0.06913	0.00129	1.40119	0.02889	0.14703	0.00229	0.50	101	902.6	37.93	884.3	12.88
74322_117	0.06036	0.00090	0.82860	0.01476	0.09958	0.00151	0.60	100	616.4	31.98	611.9	8.84
74322_118	0.05077	0.00108	0.27737	0.00640	0.03962	0.00062	0.45	99	230.6	48.6	250.5	3.87
74322_119	0.05079	0.00165	0.22158	0.00732	0.03164	0.00054	0.29	101	231.3	73.32	200.8	3.37
74322_120	0.04788	0.00371	0.11439	0.00874	0.01733	0.00038	0.09	99	92.2	174.86	110.8	2.43
74322_121	0.04981	0.00295	0.13066	0.00757	0.01903	0.00042	0.13	103	186	132.49	121.5	2.67
74322_122	0.04803	0.00112	0.11045	0.00274	0.01668	0.00027	0.42	100	100.7	54.14	106.6	1.69
74322_123	0.18982	0.00257	13.81808	0.23142	0.52801	0.00813	0.65	100	2740.6	22.11	2733	34.32
74322_124	0.05782	0.00088	0.69408	0.01257	0.08707	0.00133	0.60	99	522.7	33.3	538.2	7.87
74322_125	0.05876	0.00095	0.78229	0.01472	0.09657	0.00148	0.57	99	558.2	35.13	594.3	8.72
74322_126	0.05297	0.00195	0.25680	0.00947	0.03516	0.00064	0.25	104	327.5	81.4	222.8	3.96
74322_127	0.06018	0.00092	0.81114	0.01478	0.09776	0.00150	0.60	100	610.1	32.82	601.3	8.78
74322_128	0.08011	0.00136	2.30474	0.04476	0.20868	0.00327	0.55	99	1199.7	33.09	1221.8	17.47
74322_129	0.07674	0.00174	2.06379	0.04959	0.19505	0.00327	0.43	99	1114.6	44.59	1148.7	17.62
74322_130	0.06939	0.00119	1.38346	0.02722	0.14461	0.00226	0.55	101	910.4	35.05	870.7	12.74
74322_133	0.12475	0.00172	6.32188	0.10829	0.36756	0.00561	0.64	100	2025.3	24.22	2017.9	26.46
74322_134	0.18146	0.00408	12.12227	0.28490	0.48456	0.00905	0.45	103	2666.2	36.8	2547.1	39.3
74322_135	0.05810	0.00168	0.76373	0.02262	0.09535	0.00166	0.33	98	532.9	62.03	587.1	9.75

Analysis N	Hf176/Hf177	2 S.E.	Lu176/Hf177	Yb176/Hf177	U/Pb Age (Ma)	U/Pb Age 2σ Error	Hf_i	epsilon	2σ	T(DM) Ga	T(DM) crustal
Sample 74318											
74318-02	0.282434	0.000042	0.002067	0.076897	265.3	9.1	0.282424	-6.89	2.92	1.19	1.69
74318-06	0.282801	0.000030	0.000689	0.024532	246	7.3	0.282798	5.93	2.12	0.63	0.87
74318-08	0.281878	0.000057	0.000652	0.028453	1024.3	32.5	0.281866	-9.62	3.99	1.91	2.44
74318-12	0.282755	0.000175	0.000712	0.029122	253.5	8.2	0.282752	4.47	12.25	0.70	0.97
74318-13	0.282394	0.000070	0.001484	0.055248	312.3	11.6	0.282386	-7.19	4.93	1.23	1.75
74318-17	0.282102	0.000124	0.000902	0.031424	1444.6	45.7	0.282077	7.44	8.68	1.62	1.72
74318-18	0.282769	0.000086	0.001470	0.058458	283.4	13.1	0.282761	5.45	6.03	0.69	0.93
74318-19	0.281686	0.000082	0.000467	0.015274	1739.4	59.7	0.281671	-0.23	5.74	2.17	2.42
74318-20	0.282841	0.000047	0.000944	0.033927	109.7	3.8	0.282839	4.35	3.32	0.58	0.86
74318-23	0.283082	0.000084	0.001770	0.058978	110.4	4.1	0.283078	12.82	5.85	0.25	0.32
74318-27	0.281928	0.000114	0.000982	0.034151	1145.2	35.5	0.281906	-5.43	7.95	1.86	2.27
74318-28	0.282737	0.000055	0.001308	0.037846	320.3	10.7	0.282729	5.14	3.84	0.74	0.98
74318-32	0.282179	0.000047	0.000973	0.030310	488.8	19.7	0.282170	-10.89	3.30	1.51	2.11
74318-33	0.282920	0.000047	0.001077	0.030876	132	6.1	0.282917	7.60	3.30	0.47	0.68
74318-34	0.282316	0.000033	0.000574	0.022079	465.5	20.5	0.282311	-6.42	2.31	1.31	1.82
74318-37	0.282253	0.000078	0.000802	0.032836	1024.5	41.9	0.282238	3.59	5.44	1.40	1.63
74318-39	0.282429	0.000061	0.000728	0.028871	622.5	25.5	0.282421	1.00	4.25	1.16	1.47
74318-40	0.282132	0.000048	0.000977	0.038482	555.3	23.0	0.282122	-11.10	3.35	1.58	2.17
74318-43	0.282208	0.000040	0.001015	0.028978	601.4	15.8	0.282196	-7.43	2.78	1.47	1.98
74318-49	0.282424	0.000039	0.001495	0.050319	259	8.9	0.282417	-7.27	2.73	1.19	1.71
74318-51	0.282427	0.000057	0.000249	0.009807	514	18.8	0.282425	-1.29	4.00	1.14	1.53
74318-53	0.282403	0.000035	0.000743	0.026930	724.2	22.6	0.282393	2.30	2.44	1.19	1.47
74318-58	0.282403	0.000027	0.000467	0.015312	1139.2	34.5	0.282393	11.68	1.88	1.18	1.21
Sample 74319											
74319-02	0.282301	0.000029	0.000548	0.021515	573.7	15.2	0.282295	-4.56	2.01	1.33	1.78
74319-06	0.281959	0.000029	0.000387	0.014638	602.9	16.0	0.281955	-15.95	2.04	1.79	2.51
74319-07	0.282461	0.000020	0.000392	0.014113	527.3	13.6	0.282458	0.16	1.37	1.10	1.45
74319-10	0.281987	0.000025	0.000644	0.025825	579	15.8	0.281980	-15.58	1.76	1.76	2.47
74319-11	0.282946	0.000026	0.000616	0.023041	115	6.1	0.282945	8.21	1.80	0.43	0.62
74319-12	0.282338	0.000026	0.000997	0.034654	335.6	9.1	0.282332	-8.58	1.85	1.29	1.85
74319-13	0.281923	0.000019	0.000540	0.018999	1103.1	32.9	0.281911	-6.21	1.36	1.85	2.29
74319-15	0.281278	0.000017	0.000244	0.008570	313.8	11.1	0.281276	-46.41	1.22	2.70	4.14
74319-16	0.282233	0.000059	0.000520	0.015063	545.3	16.5	0.282228	-7.57	4.14	1.42	1.95
74319-17	0.282276	0.000016	0.000200	0.007532	554.8	23.4	0.282273	-5.74	1.09	1.35	1.84
74319-20	0.282296	0.000020	0.000355	0.015544	558.9	21.3	0.282292	-4.97	1.39	1.33	1.80
74319-21	0.282072	0.000024	0.000406	0.015528	1158.1	34.9	0.282063	0.42	1.70	1.64	1.93
74319-22	0.282278	0.000038	0.000662	0.025831	903.4	28.2	0.282267	1.86	2.67	1.36	1.64
74319-24	0.281912	0.000030	0.001519	0.049711	1566.5	58.2	0.281867	2.78	2.13	1.91	2.10
74319-25	0.282857	0.000026	0.001296	0.050330	228.4	7.6	0.282852	7.43	1.83	0.56	0.76
74319-26	0.282365	0.000070	0.001696	0.069251	687.9	18.5	0.282343	-0.28	4.88	1.28	1.60
74319-35	0.282868	0.000034	0.000887	0.030816	161.6	5.7	0.282866	6.44	2.39	0.54	0.77

	74319-37	0.282648	0.000070	0.001051	0.043886	197	6.8	0.282644	-0.60	4.91	0.86	1.25
	74319-40	0.281234	0.000069	0.000592	0.017960	2859.7	73.2	0.281201	9.14	4.85	2.79	2.75
	74319-41	0.282843	0.000069	0.001738	0.052542	107.5	5.3	0.282840	4.31	4.86	0.59	0.87
	74319-42	0.282135	0.000034	0.001127	0.037430	1152.8	35.4	0.282110	1.97	2.35	1.58	1.83
	74319-45	0.282423	0.000024	0.000452	0.018000	790.1	28.2	0.282416	4.61	1.70	1.16	1.38
	74319-48	0.282455	0.000048	0.001310	0.045812	282.3	9.6	0.282448	-5.65	3.34	1.14	1.63
	74319-51	0.282304	0.000023	0.001164	0.041777	457	15.6	0.282294	-7.18	1.64	1.34	1.86
	74319-55	0.282462	0.000023	0.000415	0.016134	609.2	22.6	0.282457	1.98	1.58	1.10	1.40
	74319-59	0.282228	0.000022	0.000293	0.011585	603.1	23.9	0.282224	-6.39	1.56	1.42	1.92
	74319-65	0.282881	0.000032	0.001069	0.035358	226.8	10.6	0.282877	8.29	2.25	0.53	0.71
	74319-66	0.281651	0.000026	0.000118	0.004335	1538.8	71.5	0.281647	-5.66	1.81	2.19	2.59
	74319-68	0.282975	0.000025	0.000497	0.018057	107.8	5.7	0.282974	9.07	1.76	0.39	0.56
	74319-69	0.282100	0.000028	0.000621	0.021440	1151.3	49.5	0.282086	1.08	1.95	1.61	1.88
	74319-77	0.282046	0.000043	0.000762	0.020826	1448.8	62.6	0.282025	5.69	3.01	1.69	1.83
	74319-78	0.282378	0.000069	0.001412	0.051862	283.4	14.0	0.282370	-8.37	4.85	1.25	1.80
	74319-80	0.282208	0.000023	0.000326	0.012285	541.8	24.6	0.282204	-8.47	1.62	1.45	2.00
Sample 74321												
	74321-03	0.282117	0.000018	0.000078	0.003569	540.3	15.6	0.282116	-11.64	1.29	1.56	2.20
	74321-08	0.282895	0.000020	0.000474	0.015389	108.3	4.9	0.282894	6.25	1.38	0.50	0.74
	74321-10	0.282776	0.000029	0.001068	0.033376	241.4	8.4	0.282771	4.86	2.01	0.68	0.94
	74321-11	0.282292	0.000015	0.000920	0.035757	802.7	20.4	0.282278	-0.01	1.04	1.35	1.68
	74321-12	0.282122	0.000126	0.000808	0.023830	1109.8	40.3	0.282105	0.81	8.82	1.59	1.86
	74321-13	0.282478	0.000057	0.000895	0.038151	590.5	18.5	0.282468	1.94	3.97	1.09	1.39
	74321-14	0.281998	0.000023	0.000157	0.005598	524.6	16.2	0.281996	-16.23	1.64	1.73	2.47
	74321-15	0.281533	0.000042	0.001203	0.045554	1942.6	49.3	0.281488	-2.03	2.97	2.42	2.68
	74321-16	0.282723	0.000028	0.000797	0.026518	240.7	7.6	0.282719	3.01	1.96	0.75	1.05
	74321-22	0.282842	0.000040	0.001659	0.062085	274	8.9	0.282833	7.79	2.80	0.59	0.77
	74321-23	0.281673	0.000040	0.000985	0.028946	193.7	6.5	0.281669	-35.18	2.78	2.21	3.38
	74321-25	0.282835	0.000022	0.001176	0.041245	269.3	10.4	0.282829	7.54	1.52	0.59	0.79
	74321-28	0.282274	0.000210	0.003511	0.118159	288.3	12.9	0.282255	-12.34	14.68	1.48	2.05
	74321-30	0.282333	0.000013	0.000034	0.001531	553.3	23.8	0.282333	-3.66	0.94	1.27	1.71
	74321-31	0.281818	0.000030	0.000909	0.032389	1535.1	107.9	0.281791	-0.64	2.07	2.01	2.28
	74321-32	0.281384	0.000018	0.000799	0.031294	1862.5	63.2	0.281356	-8.58	1.27	2.60	3.02
	74321-33	0.282421	0.000023	0.000816	0.032000	480	21.7	0.282413	-2.46	1.64	1.17	1.58
	74321-35	0.281934	0.000082	0.001108	0.029399	1158.7	43.6	0.281909	-5.02	5.73	1.86	2.26
	74321-38	0.282051	0.000015	0.000094	0.004329	544.7	27.7	0.282050	-13.88	1.08	1.65	2.34
	74321-39	0.280680	0.000089	0.000668	0.021008	2976.1	138.3	0.280642	-8.03	6.23	3.53	3.84
	74321-40	0.282055	0.000013	0.000102	0.004509	509.9	30.3	0.282054	-14.53	0.93	1.65	2.35
	74321-42	0.282778	0.000060	0.000952	0.029291	923	46.7	0.282762	19.86	4.22	0.67	0.53
	74321-44	0.282245	0.000032	0.000917	0.032002	270.4	33.2	0.282241	-13.25	2.24	1.42	2.09
Sample 74322												
	74322-01	0.282332	0.000036	0.001876	0.070944	1018	27.1	0.282296	5.51	2.50	1.33	1.50
	74322-02	0.281351	0.000021	0.000569	0.021371	493.5	14.4	0.281346	-39.94	1.46	2.63	3.88
	74322-03	0.282113	0.000022	0.000596	0.021940	1084.9	32.4	0.282101	0.10	1.55	1.59	1.89
	74322-06	0.282095	0.000020	0.000755	0.028180	1152.9	36.3	0.282079	0.86	1.37	1.62	1.89

	74322-13	0.282973	0.000024	0.000814	0.026707	131.3	4.6	0.282971	9.48	1.68	0.39	0.55
	74322-16	0.282966	0.000019	0.000496	0.018127	97.5	6.4	0.282965	8.54	1.31	0.40	0.59
	74322-18	0.282417	0.000015	0.000052	0.002429	591.5	18.1	0.282416	0.13	1.03	1.15	1.50
	74322-20	0.281932	0.000016	0.000793	0.029069	1565.1	42.5	0.281908	4.20	1.13	1.85	2.01
	74322-21	0.283008	0.000018	0.001010	0.033485	160.5	6.4	0.283005	11.33	1.24	0.35	0.46
	74322-26	0.283016	0.000019	0.000290	0.008897	100.8	8.3	0.283015	10.38	1.30	0.33	0.47
	74322-27	0.282298	0.000019	0.000885	0.033197	469.3	16.6	0.282291	-7.04	1.36	1.34	1.86
	74322-29	0.282418	0.000014	0.000052	0.002172	540.5	16.6	0.282417	-0.97	0.95	1.15	1.53
	74322-31	0.282038	0.000028	0.000614	0.021820	1134.3	36.6	0.282025	-1.49	1.99	1.69	2.02
	74322-32	0.282096	0.000018	0.001006	0.037132	1133	32.1	0.282075	0.26	1.24	1.63	1.92
	74322-40	0.281603	0.000033	0.000709	0.030707	1647.5	48.9	0.281581	-5.53	2.28	2.29	2.67
	74322-42	0.282384	0.000037	0.001446	0.045311	954.8	26.8	0.282358	6.27	2.57	1.24	1.40
	74322-45	0.282685	0.000018	0.000688	0.024691	320.8	11.4	0.282681	3.45	1.25	0.80	1.09
	74322-50	0.283020	0.000019	0.001008	0.029498	179.1	6.0	0.283016	12.16	1.36	0.33	0.42
Sample 74323												
	74323-07	0.282430	0.000038	0.000931	0.034361	1005.5	31.2	0.282413	9.34	2.65	1.16	1.25
	74323-08	0.282871	0.000025	0.001051	0.040081	100.2	6.2	0.282869	5.20	1.72	0.54	0.80
	74323-09	0.281754	0.000017	0.000128	0.005280	566.1	18.9	0.281753	-23.92	1.20	2.06	2.97
	74323-10	0.281769	0.000015	0.000120	0.004897	571.4	18.0	0.281768	-23.26	1.07	2.03	2.93
	74323-11	0.282886	0.000019	0.000551	0.019603	225.2	10.1	0.282883	8.48	1.31	0.51	0.69
	74323-12	0.282302	0.000022	0.000973	0.036387	984.7	27.2	0.282284	4.31	1.52	1.34	1.55
	74323-13	0.282175	0.000017	0.000236	0.009878	557.8	25.4	0.282173	-9.24	1.19	1.49	2.06
	74323-14	0.282176	0.000017	0.000254	0.010690	571.4	23.3	0.282173	-8.91	1.22	1.49	2.05
	74323-15	0.282386	0.000017	0.000438	0.016815	178.9	16.6	0.282385	-10.19	1.21	1.21	1.83
	74323-19	0.282274	0.000020	0.001135	0.043380	741.9	21.8	0.282258	-2.09	1.39	1.39	1.76
	74323-20	0.282292	0.000019	0.000746	0.028806	732.7	21.8	0.282282	-1.46	1.36	1.35	1.71
	74323-22	0.282396	0.000018	0.000492	0.020412	597.4	16.1	0.282390	-0.66	1.29	1.20	1.56
	74323-30	0.282988	0.000040	0.003087	0.106831	96.4	2.9	0.282983	9.13	2.81	0.40	0.55
	74323-31	0.282957	0.000036	0.001627	0.056666	95.1	4.6	0.282954	8.08	2.50	0.43	0.62
	74323-40	0.281941	0.000018	0.000512	0.019464	561.0	28.5	0.281935	-17.57	1.27	1.82	2.58
	74323-41	0.282125	0.000015	0.000130	0.005634	528.7	26.2	0.282124	-11.62	1.02	1.55	2.19
	74323-63	0.282410	0.000019	0.000721	0.029415	528.1	15.3	0.282402	-1.77	1.36	1.18	1.57
	74323-64	0.282328	0.000012	0.000051	0.002545	591.1	16.9	0.282327	-3.02	0.87	1.27	1.70
Sample 74326												
	74326-01	0.282079	0.000014	0.000134	0.004333	1261.2	38.2	0.282075	3.19	0.95	1.62	1.84
	74326-02	0.280795	0.000017	0.000853	0.029819	2684	70.7	0.280751	-10.99	1.19	3.40	3.79
	74326-03	0.282994	0.000015	0.000800	0.026683	148.2	11.3	0.282991	10.59	1.06	0.36	0.50
	74326-04	0.280963	0.000022	0.000522	0.019172	2703.6	83.8	0.280936	-3.97	1.53	3.14	3.39
	74326-08	0.282811	0.000023	0.000748	0.028824	288.7	11.5	0.282807	7.21	1.61	0.62	0.82
	74326-12	0.282461	0.000013	0.000409	0.015919	528	16.8	0.282457	0.18	0.88	1.10	1.45
	74326-14	0.282335	0.000013	0.000209	0.007813	510.3	15.1	0.282333	-4.63	0.88	1.27	1.74
	74326-16	0.281885	0.000015	0.000269	0.009787	1128.3	38.9	0.281879	-6.77	1.03	1.89	2.34
	74326-19	0.282298	0.000018	0.000443	0.016411	726.2	28.7	0.282292	-1.22	1.28	1.33	1.69
	74326-22	0.281674	0.000017	0.000251	0.009512	513.9	22.2	0.281671	-27.97	1.22	2.17	3.18
	74326-24	0.282348	0.000030	0.000439	0.013927	650.2	25.0	0.282342	-1.16	2.09	1.26	1.63

74326-25	0.282161	0.000018	0.000444	0.017471	895	32.9	0.282153	-2.34	1.28	1.52	1.89
74326-26	0.282321	0.000011	0.000046	0.002167	558.8	24.4	0.282320	-3.99	0.77	1.28	1.74
74326-31	0.283025	0.000020	0.000816	0.024894	98	4.7	0.283023	10.60	1.41	0.32	0.46
74326-34	0.282423	0.000026	0.001555	0.059029	358.5	12.8	0.282413	-5.20	1.81	1.19	1.66
74326-38	0.282476	0.000025	0.001273	0.045205	302.6	11.3	0.282468	-4.48	1.73	1.11	1.57
74326-41	0.282795	0.000021	0.000715	0.023437	241.5	8.4	0.282792	5.61	1.46	0.64	0.89
74326-42	0.282338	0.000011	0.000027	0.001200	565.5	19.5	0.282338	-3.21	0.74	1.26	1.69
74326-43	0.282818	0.000084	0.001694	0.044654	242.7	8.5	0.282811	6.30	5.87	0.63	0.84
74326-44	0.282378	0.000020	0.000178	0.007010	651.1	24.5	0.282376	0.06	1.38	1.21	1.55
74326-45	0.282290	0.000018	0.000030	0.001408	503.7	18.0	0.282290	-6.29	1.25	1.32	1.84
74326-46	0.282273	0.000022	0.000822	0.028373	771.7	28.0	0.282261	-1.30	1.56	1.38	1.73
74326-50	0.282510	0.000019	0.000379	0.013613	537.5	19.5	0.282506	2.12	1.33	1.03	1.34
74326-51	0.280724	0.000025	0.000225	0.007927	2370.3	91.6	0.280714	-19.63	1.76	3.43	4.05
74326-53	0.281766	0.000014	0.000416	0.015929	558.4	23.4	0.281762	-23.77	0.97	2.05	2.95
74326-55	0.282403	0.000014	0.000110	0.003775	530.9	19.6	0.282402	-1.73	1.01	1.17	1.57
74326-57	0.282366	0.000032	0.000047	0.001754	503.9	22.2	0.282366	-3.61	2.21	1.22	1.67
74326-60	0.282532	0.000025	0.002011	0.074911	285.8	11.2	0.282521	-2.99	1.75	1.05	1.47
74326-61	0.281680	0.000055	0.001303	0.036228	1649.4	52.2	0.281640	-3.39	3.85	2.22	2.54
74326-66	0.282212	0.000026	0.000591	0.024845	685.4	19.8	0.282204	-5.27	1.80	1.45	1.91
74326-71	0.282741	0.000070	0.001086	0.038287	242.8	10.7	0.282736	3.68	4.87	0.73	1.01
74326-72	0.282304	0.000032	0.000433	0.016254	765.7	21.9	0.282298	-0.14	2.21	1.32	1.66
74326-77	0.281398	0.000052	0.000948	0.034428	1856.7	50.2	0.281365	-8.39	3.67	2.59	3.00
74326-78	0.282434	0.000021	0.001334	0.050635	244.1	12.0	0.282428	-7.22	1.48	1.17	1.70
74326-79	0.282261	0.000035	0.000692	0.030204	803.9	24.9	0.282251	-0.94	2.43	1.39	1.73

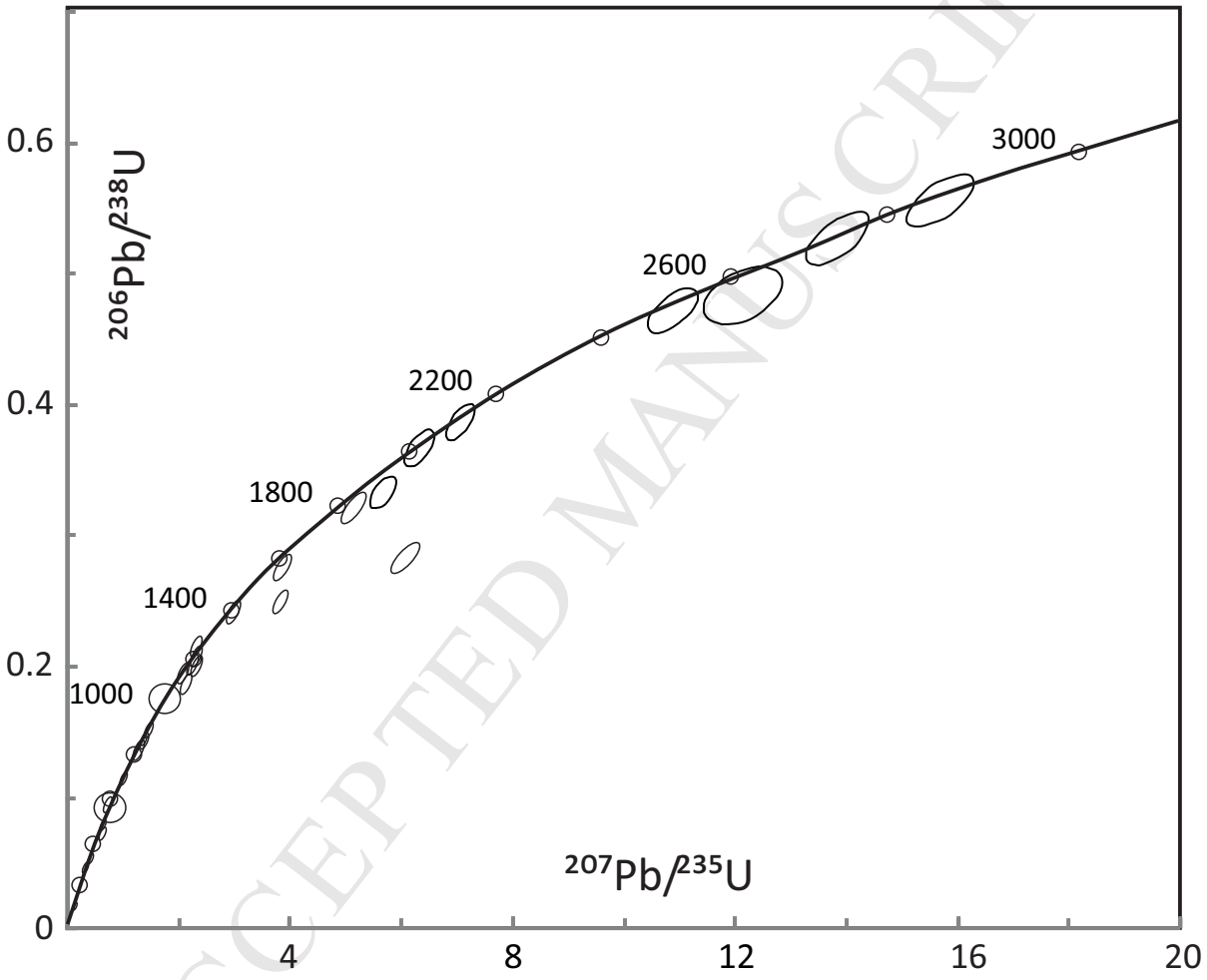

Supplementary Figure